Table 2.5.3.14. *Diffraction groups and CBED symmetries for two icosahedral point groups*

| Point group | Diffraction group | BP | WP | DP | ±DP |
|---|---|---|---|---|---|
| 235 | $5m_R$ | $5m$ | 5 | 1 | 1 |
| | | | | | $m_R$ |
| | | | | $m_2$ | 1 |
| | (Projection) $5m1_R$ | $10mm$ | $5m$ | $2 = 1_R$ | 1 |
| | | | | | $m_v1_R$ |
| | | | | $2m_vm_2$ | 1 |
| $m\bar{3}\bar{5}$ | $10_Rmm_R$ | $10mm$ | $5m$ | 1 | $2_R$ |
| | | | | $m_2$ | $2_Rm_2$ |
| | | | | $m_v$ | $2_Rm_v$ |
| | (Projection) $10mm1_R$ | $10mm$ | $10mm$ | 2 | $21_R$ |
| | | | | $2m_vm_2$ | $21_Rm_v$ |

dimensions (*e.g.* Jarić, 1988). A quasicrystal is produced by the intersection of the six-dimensional crystal with an embedded three-dimensional hyperplane (the cut-and-projection technique).

Addition of several per cent of silicon to Al–Mn alloys caused a great increase in the degree of order of the quasicrystal. Bendersky & Kaufman (1986) prepared such a less-strained quasicrystalline $Al_{71}Mn_{23}Si_6$ alloy and determined its point group. They obtained fairly good zone-axis CBED patterns that showed symmetries of $10mm$, $6mm$ and $2mm$ in the ZOLZ discs and $5m$, $3m$ and $2mm$ in HOLZ rings. From these results, they identified the point group to be centrosymmetric $m\bar{3}\bar{5}$. Figs. 2.5.3.24(*a*)–(*f*) show three pairs of CBED patterns taken from an area about 100 nm thick and about 3 nm in diameter of an $Al_{74}Mn_{20}Si_6$ quasicrystal at an accelerating voltage of 60 kV (Tanaka, Terauchi & Sekii, 1987). This quasicrystal was found to have much better ordering than $Al_{71}Mn_{23}Si_6$. The fact that Kikuchi bands are clearly seen in the HOLZ patterns and the profiles of the bands are symmetric with respect to their centre indicates (Figs. 2.5.3.24*b*, *d* and *f*) that the quasicrystal has sufficiently good quality or highly ordered atomic arrangements to perform reliable symmetry determination. Each pair of CBED patterns consists of a ZOLZ pattern and a HOLZ pattern. The former is produced solely by the interaction of ZOLZ reflections, showing distinct symmetries in several discs.

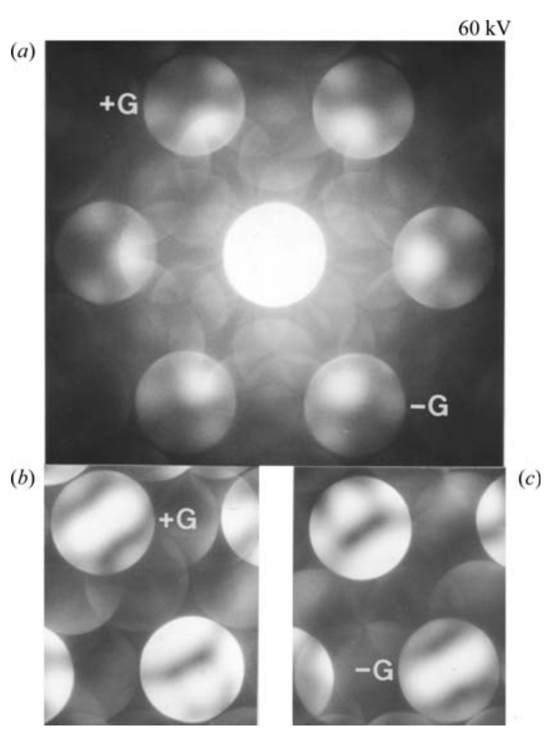


Fig. 2.5.3.25. CBED patterns of $Al_{74}Mn_{20}Si_6$ taken with an electron incidence along the threefold axis. (*a*) Zone-axis pattern showing symmetry $3m$. (*b*,*c*) ±DP showing translational symmetry or $2_R$, indicating that the quasicrystal is centrosymmetric.

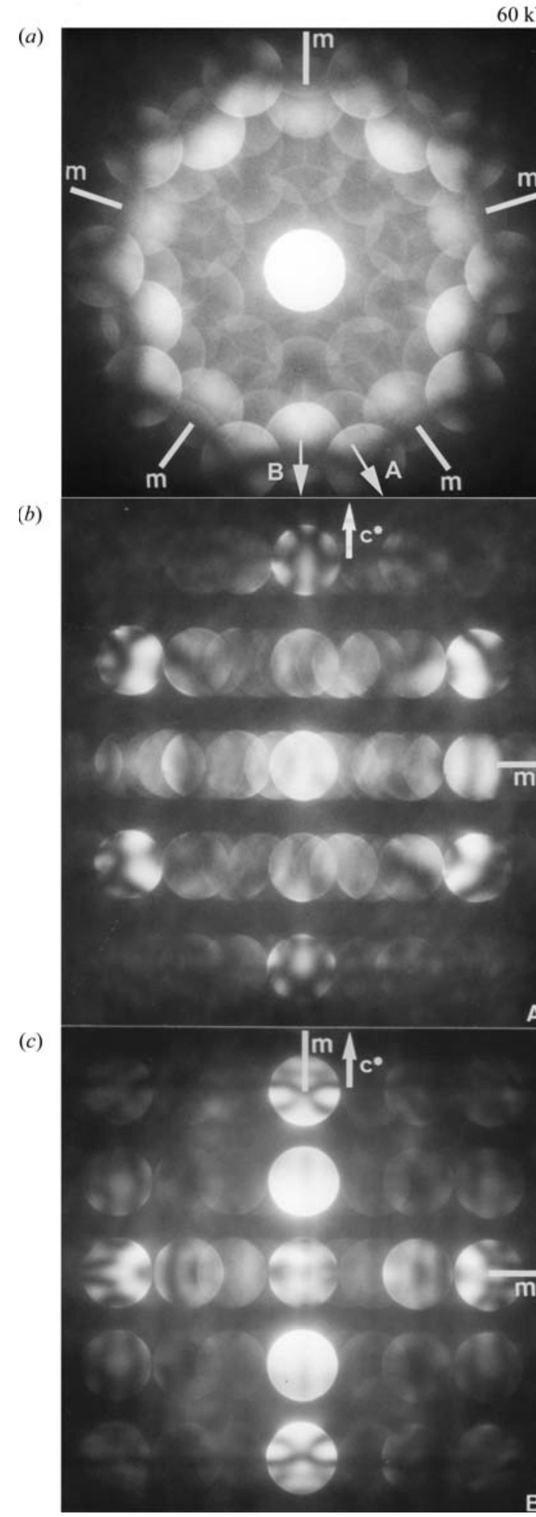


Fig. 2.5.3.26. CBED patterns of metastable $Al_{70}Ni_{15}Fe_{15}$ taken from a 3 nm diameter area. (*a*) Electron incidence along the decagonal axis: symmetry $5m$. (*b*) Electron incidence along direction A indicated in (*a*): symmetry $m$ perpendicular to the decagonal axis. (*c*) Electron incidence along direction B indicated in (*a*): symmetry $2mm$. This alloy is found to be noncentrosymmetric.

The whole pattern of Fig. 2.5.3.24(*a*), formed by ZOLZ reflections, exhibits a tenfold rotation symmetry and two types of mirror symmetry, the resultant symmetry being expressed as